**International Journal of Reconfigurable and Embedded Systems (IJRES)**
Vol. 15, No. 3, November 2026, pp. 878~888
ISSN: 2089-4864, DOI: 10.11591/ijres.v15.i3.pp878-888 

# Design of a compact wideband slotted microstrip patch antenna for Sub-6 GHz 5G internet of things systems

**Arputham Jenifer[1], Chinnasamy Mohan[2], Sasidharan Sandhya[3], Anbarasu Muthu Manickam[4], Ravindran Sornalatha[5], Balasundaram Jothi[6]**

[1]Department of Artificial Intelligence and Data Science, St. Joseph's Institute of Technology, Chennai, India
[2]Department of Electronics and Communication Engineering, St. Joseph's Institute of Technology, Chennai, India
[3]Department of Artificial Intelligence and Data Science, Easwari Engineering College, Chennai, India
[4]Department of Electronics and Communication Engineering, Shanmuganathan Engineering College, Pudukkottai, India.
[5]Department of Electrical and Electronics Engineering, Mount Zion College of Engineering and Technology, Pudukkottai, India
[6]Department of Computational Intelligence, SRM Institute of Science and Technology, Kattankulathur, India

**Article Info**

***Article history:***

Received Feb 20, 2026
Revised Jun 22, 2026
Accepted Jul 18, 2026

***Keywords:***

Inset feed
Miniaturization
Slot antenna
Sub-6 GHz applications
Wideband

**ABSTRACT**

The article describes an extremely small wideband slotted rectangular patch antenna that is suitable for Sub-6 GHz applications in modern wireless broadband networks. The suggested antenna is fabricated on a FR-4 substrate and has small dimensions of 15 mm ×12 mm ×1.6 mm (88% miniaturization when compared to conventional antenna for 3.6 GHz). By adding two rectangular slots to the radiating patch, miniaturization is accomplished while preserving the antenna's total size unchanged. In order to achieve wideband characteristics, which span a frequency range of 3.1 GHz to 6.6 GHz and approximate to a 3.5 GHz bandwidth (70.8% fractional bandwidth), the inset feed approach and rectangular slots are used. The antenna has excellent impedance match, consistent radiation properties, having a peak gain of 2.77 dB. The evaluations show that the constructed antenna has a high gain, strong radiation performance, and is in good correlation with the computed results. A fabricated prototype has been assessed and experimentally validated to ensure that the proposed antenna is appropriate for portable wireless equipment and Sub-6 GHz 5G applications.

*This is an open access article under the CC BY-SA license.*

***Corresponding Author:***

Chinnasamy Mohan
Department of Electronics and Communication Engineering, Faculty of Engineering
St. Joseph's Institute of Technology
Chennai 600119, Tamil Nadu, India
Email: mohanrc803@gmail.com

## 1. INTRODUCTION

Because of its great capabilities in terms of coverage, signal penetration, and data throughput, the Sub-6 GHz frequency range has become one of the essential components of modern wireless communication technology. In Wi-Fi, the internet of things (IoT), and 5G mobile communication technologies, where constant connectivity is crucial, frequencies below 6 GHz are widely utilized [1], [2]. In particular, this frequency range is crucial for connectivity in the context of 5G technology's massive machine-type communications (mMTC) and enhanced mobile broadband (eMBB) services, which enable effective long-distance connectivity for numerous devices. The Sub-6 GHz range has reduced propagation loss in comparison to millimeter-wave frequencies, allowing for steady operation in both indoor and outdoor settings. This makes it highly suitable for IoT-based applications such as smart homes, industrial automation, autonomous vehicles, and remote healthcare monitoring systems.

Antennas designed for use in IoT-based 5G technology are essential components that provide dependable wireless communications between numerous devices. For example, small size, wide bandwidth, and consistent radiation performance for various IoT systems are important factors for antennas in Sub-6 GHz bands, particularly those at 3.5 GHz frequencies [3]. Because of their comparatively low weight and profile, these antennas can be used in a variety of small devices, such as wearable electronics, smart modules, and sensors. While effective impedance matching helps to ensure minimal signal losses, wide bandwidth is necessary to operate at high speeds and employ various communication standards. The most common methods for expanding an antenna's bandwidth and reducing its size are miniaturization and defective ground structure (DGS) [4]. 5G IoT antennas are therefore made to meet the demands of contemporary users.

An antenna configuration for the 5G IoT network still faces a number of technical obstacles despite tremendous progress. One of the most significant challenges facing designers is the requirement to minimize the number of antennas while preserving exceptional performance in respect to gain, high efficiency, and wide bandwidth. Particularly when combined with low-cost materials, miniaturized antennas typically have poor radiation efficiency and greater loss values. Maintaining radiation patterns and broadband performance is another issue in antenna development. The trade-off between size and performance is the cause of this problem. Additionally, many IoT devices are utilized in crowded areas, which leads to electromagnetic interference and coupling [5]. Recently, one of the main issues with wireless technologies has been antenna downsizing. As the antenna dimensions are reduced, it becomes more challenging to maintain the required radiation efficiency, impedance matching, and gain behavior. Miniaturization results in a smaller operating bandwidth because of the decrease in effective aperture and the quantity of energy that can be stored in a compact structure [6]. To achieve wideband properties in such a small structure, careful form, feeding strategy, and substrate design is necessary. Several strategies, including slot loading, DGS, metamaterials, and parasitics, are used to get around these challenges [7]-[9]. Nevertheless, these methods make antenna manufacture, tuning, and performance stability even more difficult. In addition to these factors, dielectric losses have an impact on smaller antennas' efficiency. In antenna engineering, striking a balance between compactness and bandwidth increase is still a major research challenge. For the next generation of wireless networks, it is therefore essential to create innovative design techniques that integrate broadband operation with miniaturization.

The integration and performance requirements of Sub-6 GHz 5G and IoT devices have led to the development of several small antenna configurations. A compact footprint of about 25 mm ×20 mm ×1.6 mm and a wide operating range of 3.3 GHz to 4.2 GHz are achieved by a tiny printed antenna on a FR-4 surface featuring a slotted partial surface [10]. A coplanar waveguide (CPW) feed and optimized monopole geometry allowed for the downsizing of a flexible four-element multiple input multiple output (MIMO) antenna that measures 66 mm ×66 mm ×0.13 mm and operates between 3.2 GHz and 4.12 GHz [11]. Using inverted-L branches and shorting pins to save space, this twelve-element dual-band antenna for smartphones covers 3.32–3.61 GHz and 4.75–5.05 GHz with individual element heights of just 3 mm and element spacing of 3 mm [12]. A planar slot antenna can operate in two bands (3.2–3.6 GHz and 4.2–5.1 GHz) in a small area of approximately 0.3 $\lambda_o$×0.17 $\lambda_o$ (approximately 28 mm ×16 mm at 3.3 GHz), using slot and folded T-stub mounting to expand the current path [13]. A semicircular slot antenna with DGS that achieves dual-band coverage in the Sub-6 GHz region while realizing a compact size of roughly 20 mm ×18 mm [14]. All of these experiments demonstrate the great effectiveness of slot loading, folded-stub feeds, flexible substrates, and DGS topologies in producing tiny yet wideband antennas.

To achieve a bandwidth of about 700 MHz in the 3.3–4.2 GHz range, the scientists used a partially slotted ground plane beneath a modified patch fed by a basic feedline. A four-port MIMO antenna with an L-shaped element and ground plane slots provided wide-band matching from 3.2–5.6 GHz (~54% fractional bandwidth) through structural arrangement and slot coupling [15]. By using an inset-coupled feed instead of a probe or standard line, the triangle-shaped patch antenna in [16], a small inset coupling feed with triangular patch antenna for broadband 5G applications, improved feed-point impedance management and increased matched bandwidth. A dipole-based radiator with loop-branch and short-circuit L-shaped feed branches obtained a wide band covering 3.3–3.8 GHz (and filtering undesirable bands) with a specifically constructed feed network in [17] a novel wideband filtering antenna for Sub-6 GHz. Lastly, a monopole on FR-4 with a feed that included a frequency-selective surface (FSS) layer behind the feed line produced impedance broadening and bandwidth improvement via feed-FSS coupling in [18] a efficient Sub-6 GHz 5G antenna with FSS addition.

In order to solve the main issues with antenna design for 5G IoT applications, slot loading techniques are crucial. Miniaturizing the antenna is necessary, but it must also have adequate bandwidth, gain, and efficiency. This can be difficult because there is a trade-off between antenna performance and size. Slot loading can alter the electrical length and surface current distribution, enhancing bandwidth and impedance matching, by creating slots in the radiating patch in various forms. This feature makes it particularly helpful for Sub-6 GHz IoT devices, which require robust wideband operation in order to offer dependable connectivity.

Additionally, slot loading can assist make the antenna wideband or multiband without significantly altering its size, which is crucial when an IoT device uses multiple frequencies.

This research proposes a broadband slotted rectangular patch antenna for wireless applications with bandwidths lower than 6 GHz. The antenna is built with a FR-4 surface and measures 15 mm ×12 mm ×1.6 mm. The research is novel since it optimizes dual-slots with an inset feed layout, resulting in an impressive reduction ratio of 88% and a fractional bandwidth of 70.8%. Compared to other designs, the suggested antenna has a high bandwidth/size ratio and good radiation and impedance characteristics. The remaining portion of this investigation is therefore given as followed. The suggested antenna's configuration is shown in section 2. Computation and test results are covered in section 3. Section 4 contains a brief review of the paper.

## 2. DESIGN METHOD

The specifications for the design of Sub-6 GHz 5G IoT applications have been met by a methodical approach to antenna design. The first rectangular patch antenna was created using fundamental design concepts, and its downsizing was accomplished by adding two slots to the radiating patch. Despite the antenna's small physical dimensions, the use of slots increases the effective current route and allows for the achievement of numerous resonances, which improves the bandwidth. Impedance matching of the design has been accomplished without the need for an additional matching network by employing the inset feed method. The design process used for the suggested antenna, from requirement specification to design validation, is shown in Figure 1. The design parameters, including operating frequency, small size, and IoT-related specifications, were established at the outset. A basic rectangular patch antenna design has been developed based on the specified specifications. The idea of slots has been used to change the antenna's current distribution and produce more resonances in order to achieve downsizing and bandwidth improvement. The feed's position was then altered in order to complete the feed optimization process. Finally, the antenna is fabricated and experimentally validated to verify its performance, ensuring that the proposed design meets the requirements of Sub-6 GHz 5G IoT applications.

Figure 2 depicts a rectangle-shaped patch antenna construction with all of its design specifications clearly indicated. The FR-4 board used for constructing the antenna has an optimal thickness of 1.57 mm. The backing material measures 15 mm by 12 mm (WS×LS). The rectangular radiating patch in the substrate's center measures 7.4 mm (LP) long by 11 mm (WP) breadth. Two rectangular slots measuring 3.8 mm by 4.8 mm (W1×L1) were etched on both sides of the patch to improve bandwidth and compactness. The feedline that excites the patch is an inset microstrip feed with dimensions of 1.75 mm (WF) by 4.15 mm (LF), which ensures adequate impedance match between the feeding line and the patch's surface area. The copper radiating and feed elements are represented by the orange section, while the FR-4 substrate is represented by the blue-colored portion.

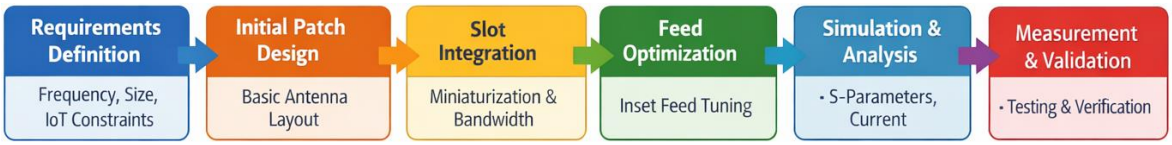



Figure 1. Workflow diagram of slotted rectangular patch antenna design

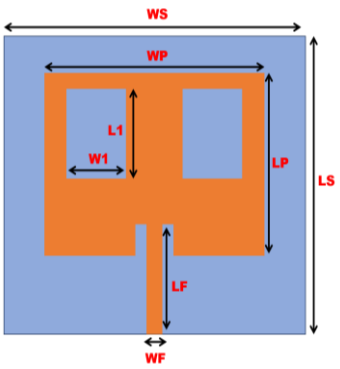
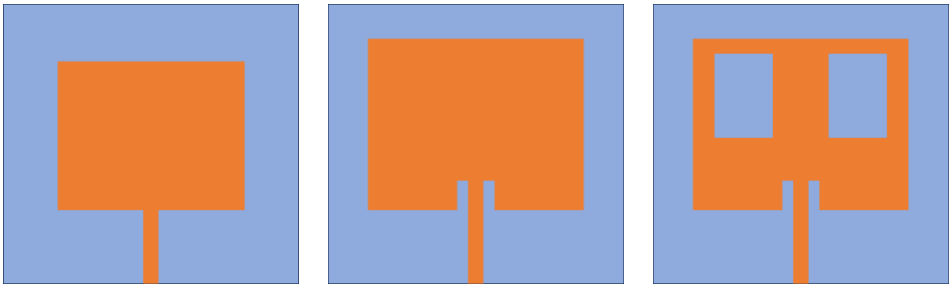



Figure 2. Total geometry and configuration of the proposed antenna

Figure 3 displays the development of the designed antenna configuration and its corresponding estimated reflection coefficients. In the initial step (Level 1), the antenna's structure is a simple rectangular radiated patch connected to a microstrip feedline. The typical antenna configuration comprises of a rectangular patch situated on a dielectric surface. The antenna's resonance frequency can be determined utilizing the corresponding (1) [19].

$$f_r = \frac{c}{4\pi L_{eff}\sqrt{\varepsilon_{eff}}} \quad (1)$$

This equation uses $f_r$ as the resonant frequency, $c$ as the speed of light in a vacuum, $L_{eff}$ as the optimum length, and $\varepsilon_{eff}$ as the material's effective permittivity. This basic structure resonates at a single frequency about 4.5 GHz, as seen in the black $S_{11}$ curve. However, it offers narrow bandwidth and poor impedance matching due to restricted surface current channels and a lack of structural tuning elements (Figure 3(a)). In the second stage (Level 2), two narrow slots are cut into the lower portion of the patch near the feedline (Figure 3(b)). These notches effectively modify the current flow and generate a new resonant mode, which improves impedance matching and increases bandwidth. Two rectangular slots are imprinted on the patch's inner surface in the third and last stage (Level 3), resulting in a more intricate current distribution that greatly improves electromagnetic coupling and enables several resonant modes. Figure 3(c) displays a red $S_{11}$ curve with deeper and larger resonances ranging from 3.1–6.6 GHz, indicating significant increase in bandwidth and return loss performance. Figure 4 depicts the relevant reflection coefficients for the recommended design's evolution.



(a) (b) (c)

Figure 3. Step-by-step evolution; (a) initial structure (Level 1), (b) intermediate structure (Level 2), and (c) final structure (Level 3)

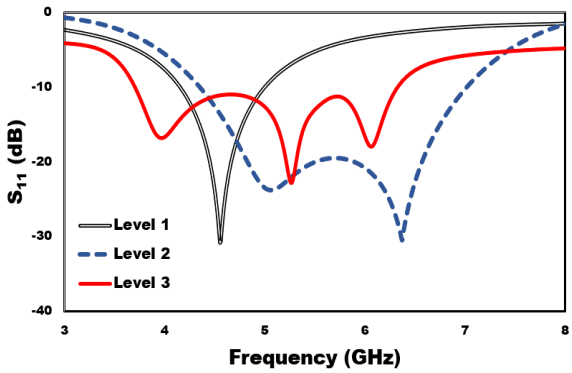
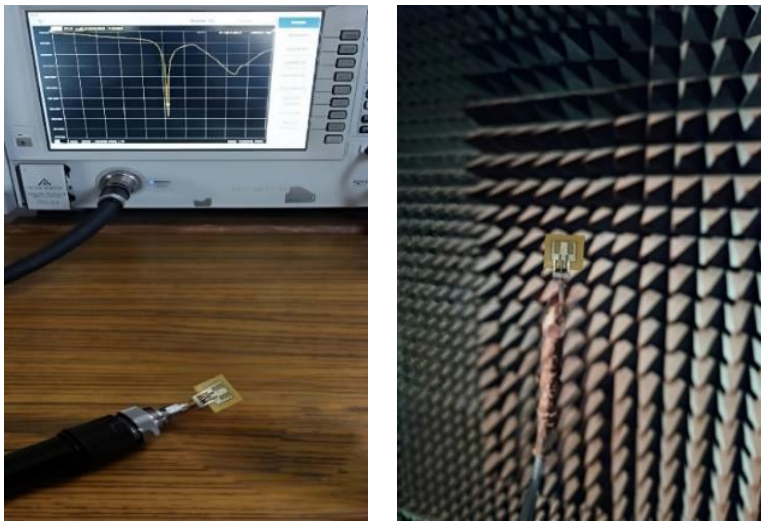



Figure 4. The evolution stages of simulated reflection coefficient ($S_{11}$)

## 3. RESULTS AND DISCUSSION

The manufactured design's performance, including bandwidth and normalized gain, is evaluated using an agilent vector network analyzer (VNA) has been depicted in Figure 5. Figure 5(a) illustrates the simulated antenna's reported reflection coefficient with impedance bandwidth, that have been measured utilizing a microwave network analyser. The working model has been examined in an anechoic chamber, as illustrated in Figure 5(b), to confirm its electromagnetic radiation and impedance characteristics.



(a) (b)

Figure 5. Antenna measurement setups used for performance validation; (a) reflection coefficient measurement with a VNA and (b) radiation pattern assessment in an anechoic environment

The anechoic chamber is used to assess radiation analysis performance. Cable loss and manufacturing tolerance accounted for most of the minor differences between the modeling and measurement results, which agree well. The amount of incident energy returned as a result of an impedance mismatch between the transmission network and antenna is measured by the reflection coefficient ($S_{11}$). A lower reflection coefficient states superior impedance match, allowing for maximum power transmission with less signal loss. The constructed proposed slotted rectangular patch antenna is 15 mm ×12 mm ×1.6 mm in total. The antenna is intended to increase bandwidth and compactness for Sub-6 GHz platforms.

### 3.1. Reflection coefficient

Figure 6 shows graphs of the evaluated and computed values of the $S_{11}$ reflection property for the frequency range of 3–8 GHz. The $S_{11}$ parameter, which indicates more power reception and less signal reflection, is used to describe impedance matching. Three resonance peaks with quite similar forms can be seen on both plots at 4, 5.5, and 7 GHz. However, the measured values (shown in red and dashed) frequently reach deeper minima at -26 dB rather than the anticipated near -20 dB, in contrast to the predicted values. Specifically, both responses are nearly equal at 3 GHz and nearly identical at -5 dB. However, there are variations in the values in high-frequency regions, which can be linked to manufacturing variations and component constraints that are not considered in simulations. There is excellent impedance matching in the frequency band of 5 to 6.5 GHz, where reflection dips are far deeper than anticipated.

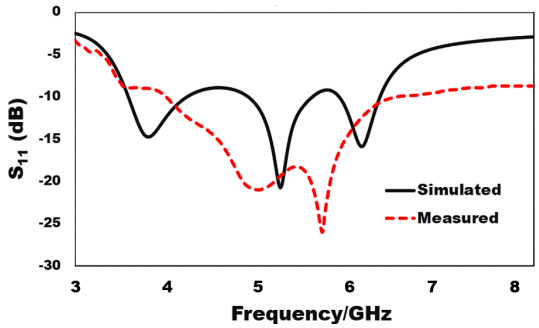
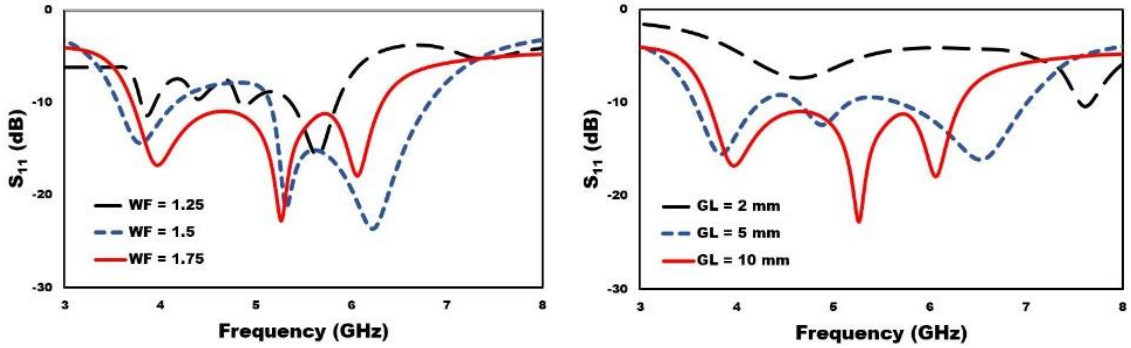



Figure 6. Comparison graph of S-parameter of the proposed antenna in both simulation and measurement

In order to examine the impact of impedance matching on feed width (WF) and ground length (GL), Figure 7 plots the fluctuation of the reflection coefficient ($S_{11}$) against frequency with various structure

parameters. Increasing the WF changes the resonance spots and improves impedance matching at specific frequencies, as seen in Figure 7(a). WF=1.75 mm results in deeper nulls that suggest lower return loss and increased resonance around mid-band. This demonstrates how a broader feed improves the coupling between the radiating component and feed line. The bandwidth and resonance in Figure 7(b) are significantly influenced by the GL; an increase in GL leads to additional resonances and reduced return losses at specific frequencies, particularly at GL=10 mm. All things considered, both factors are essential for fine-tuning the antenna's performance; ideal values lead to increased bandwidth and better impedance matching over the targeted frequency range.

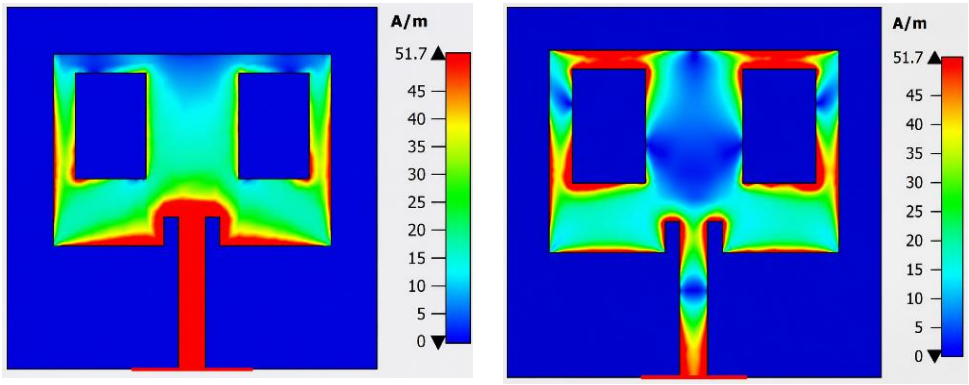



(a) (b)

Figure 7. Reflection coefficients under different operating conditions; (a) parametric study of feed width and (b) GL

### 3.2. Surface current analysis

Figure 8 displays the current density dispersion for every frequency, which can be used to analyze the antenna's function. At 3.6 GHz (Figure 8(a)), there is a strong concentration of current in the feed mechanism and around the perimeters of the slots, whereas the interiors of the slots are largely inactive. This indicates basic-mode operation, where energy effectively couples across boundary routes. The central gap between slots and improved peripheral coupling are two areas that are activated by current redistribution at 6.2 GHz (Figure 8(b)), demonstrating higher-order mode emergence where more electromagnetic pathways get electrified. The enhanced impedance matching at higher frequencies can be explained by the shift from confined perimeter currents to diffused multi-region patterns, as the antenna simultaneously takes advantage of several resonant routes to produce deeper $S_{11}$ results. This frequency-dependent current evolution shows how the dual-slot structure enables different operational modes that together result in the deeper and sharper reflection minima seen in measured data, especially in the 5–6.5 GHz area where mid-band efficiency peaks.




(a) (b)

Figure 8. Surface current density of the proposed grid array antenna; (a) 3.6 GHz and (b) 6.2 GHz

### 3.3. Radiation pattern

Figure 9 illustrates the antenna's functionality across both XOZ-plane and YOZ-plane orientations utilizing modelled two-dimensional radiation patterns at 3.6 GHz and 6.2 GHz, correspondingly. Strong polarization is evident in the correlated curves at both frequencies, particularly in the XOZ plane where sidelobe interference is negligible and the main lobe is well delineated in Figure 9(a). The angular dispersion of the YOZ-plane co-polarized response is greater in Figure 9(b). It is evident that the antenna offers a roughly omnidirectional and bidirectional pattern across both dimensions at all frequencies.

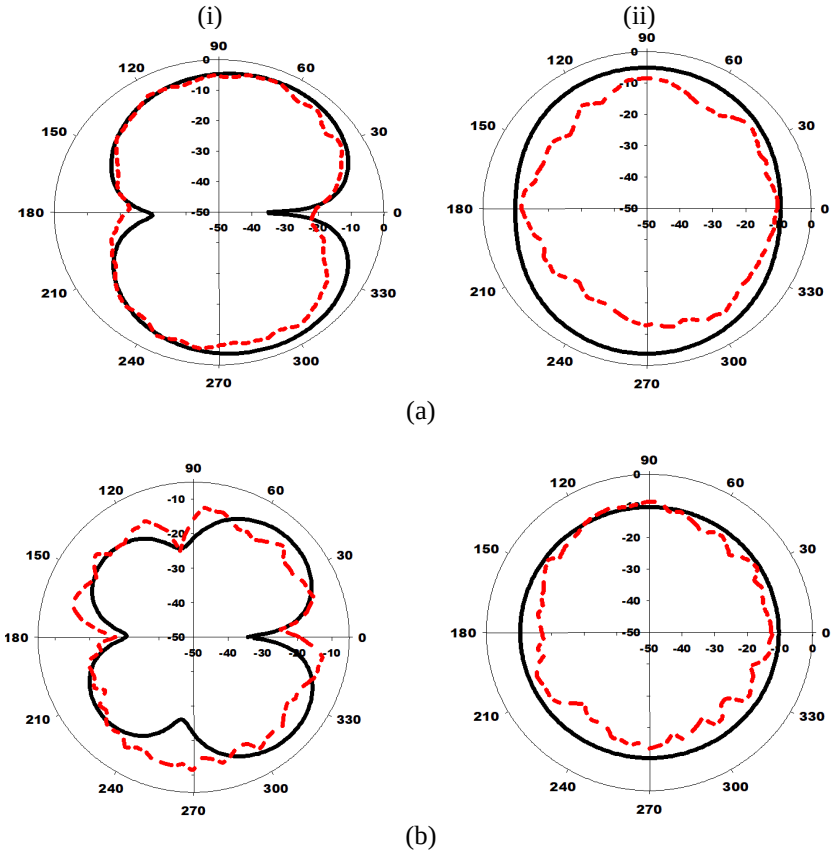



Figure 9. Measured and simulated 2D radiation pattern results of the antenna in the (i) E-plane and (ii) H-plane at frequencies of; (a) 3.6 GHz and (b) 6.2 GHz

### 3.4. Radiation efficiency and peak gain

For both simulated and details observed, the antenna behavior spanning 3.1–6.6 GHz exhibits a peak gain of roughly 2.77 dB near 4.5–5 GHz is shown in Figure 10. The measured gain exhibits minor variations but comparable overall levels, whereas the simulated gain stays constant. There is a more pronounced difference in radiation efficiency (red curve), with measured values typically 8–10% greater than simulated ones. The measured efficiency exceeds the expected range of 72–75%, peaking at about 82% close to 5 GHz and remaining above 75% between 4–5.5 GHz. Reduced performance at higher frequencies is indicated by a reduction in both gain and efficiency toward 6 GHz. Greater impedance matching attained during fabrication, which improves the transfer of energy from the feed to the radiating elements, is responsible for the increased observed efficiency.

The conventional antenna, with a larger size of 45×35 mm², operates at 3.6 GHz but provides a relatively narrow bandwidth of 0.7 GHz, indicating limited frequency coverage. By introducing slot loading without an inset feed, the antenna size is significantly reduced to 22×16 mm², achieving approximately 72% miniaturization, while the bandwidth is substantially improved to 2.8 GHz due to the creation of additional resonant modes. Miniaturization is typically calculated by comparing the proposed antenna size with a conventional reference antenna for 3.6 GHz.

$$\text{Miniaturization (\%)} = \frac{\text{Area of the Conventional Antenna} - \text{Area of the Proposed Antenna}}{\text{Area of the Conventional Antenna}} \times 100$$

$$= \frac{1575-180}{1575} \times 100 = 88.6\%$$

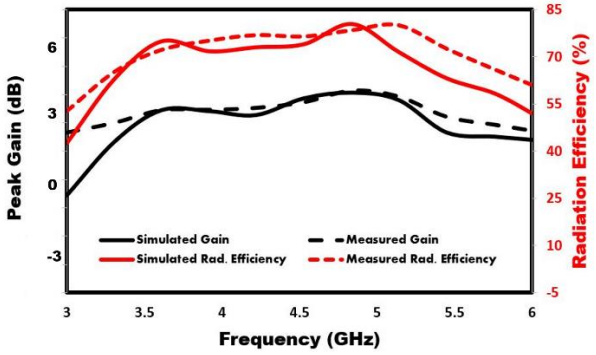



Figure 10. Variation in the designed slotted antenna's peak gain and radiation efficiency

### 3.5. Performance comparison

A comparison of the suggested antenna with previously published wideband miniaturized designs for Sub-6 GHz applications is shown in Table 1. The proposed work achieves the highest miniaturization of 88.1% with a compact electrical size of 0.24 $\lambda_0 \times 0.19 \lambda_0$, while maintaining a larger bandwidth of 3.1–6.6 GHz and a maximal fractional bandwidth of 70.8%, outperforming most existing designs. In comparison, Ucar *et al.* [20] offers a compact size but is limited by a very narrow bandwidth (6.05%), whereas Mohan *et al.* [21] provides relatively wideband performance (66%) with lower miniaturization. Designs in [22], [23] demonstrate multi-band characteristics, but they either exhibit moderate bandwidth or larger antenna dimensions, with [23] achieving higher gain at the expense of size. Similarly, Nafi *et al.* [24] shows limited gain and moderate bandwidth despite using an FR-4 substrate, and Desai *et al.* [25] provides reasonable bandwidth but lacks miniaturization data and has a comparatively larger electrical size. The suggested antenna is a competitive option for contemporary Sub-6 GHz wireless and IoT applications since it provides an enhanced trade-off between compact size, wideband operation, and consistent gain.

Table 1. Comparison with previously published wideband miniaturized antennas for Sub-6 GHz band

| Reference | Antenna size ($\lambda_0$) | Miniaturization (%) | Substrate used | Bandwidth (GHz) | Fractional bandwidth (%) | Peak gain (dB) |
|---|---|---|---|---|---|---|
| **This work** | **0.24×0.19** | **88.1** | **FR-4** | **3.1–6.6** | **70.8** | **2.77** |
| Ucar *et al.* [20] | 0.26×0.26 | 83.0 | Arlon | 3.37–3.58 | 6.05 | 2.97 |
| Mohan *et al.* [21] | 0.33×0.28 | 76.2 | FR-4 | 2.8–5.6 | 66 | 2.95 |
| Ullah *et al.* [22] | 0.40×0.42 | 57.2 | Rogers RO4003 | 3.2–37 and 5.7–6.1 | 14.5 and 6.8 | 2 and 3.24 |
| Saeidi *et al.* [23] | 0.35×0.70 | 35.7 | Denim and PTFE | 3.25–3.65 and 5.4–5.85 | 11.6 and 8.0 | 7.2 |
| Nafi *et al.* [24] | 0.56×0.54 | 21.0 | FR-4 | 3.3–4.2 and 4.4–5 | 24 and 12.8 | 0.05 and 1.88 |
| Desai *et al.* [25] | 0.54×0.72 | - | PET | 3.89–5.90 | 41.1 | 3 |

## 4. CONCLUSION

Considering a reduction of about 88%, the developed small slotted rectangular patch antenna shows a good degree of minimization. Additionally, the antenna exhibits strong performance with effective wideband characteristics across the 3.1–6.6 GHz operational frequency range. Over the operating frequency range, the proposed antenna has a return loss of less than −10 dB and a sufficient observed fractional bandwidth of approximately 70.8%. With a pleasant radiation pattern and an average gain of 2.77 dB, the built antenna validates the concept with satisfactory agreement among simulated and real measurements. Despite the antenna's exceptional performance, the FR-4 substrate used in the design shows some loss, which reduces the proposed patch antenna's overall efficiency. The current design cannot be used to achieve frequency reconfiguration or boost the gain of the patch antenna. The approach is an appropriate choice for a variety of embedded systems, wearable technology, reconfigurable devices, very large scale integration (VLSI)-based

communication systems, and other emerging wireless communication technologies due to its superior performance and effective wideband characterization.


## FUNDING INFORMATION

Authors state no funding involved.


## AUTHOR CONTRIBUTIONS STATEMENT

This journal uses the Contributor Roles Taxonomy (CRediT) to recognize individual author contributions, reduce authorship disputes, and facilitate collaboration.

| Name of Author | C | M | So | Va | Fo | I | R | D | O | E | Vi | Su | P | Fu |
|---|---|---|---|---|---|---|---|---|---|---|---|---|---|---|
| Arputham Jenifer | ✓ | ✓ | ✓ | ✓ | ✓ | ✓ | | ✓ | ✓ | | | | ✓ | |
| Chinnasamy Mohan | | ✓ | ✓ | | ✓ | ✓ | ✓ | ✓ | ✓ | | ✓ | | ✓ | |
| Sasidharan Sandhya | | ✓ | ✓ | ✓ | | | ✓ | | ✓ | | ✓ | | | |
| Anbarasu Muthu Manickam | | ✓ | | ✓ | ✓ | ✓ | | ✓ | | ✓ | | ✓ | | ✓ |
| Ravindran Sornalatha | | ✓ | | ✓ | ✓ | ✓ | ✓ | | ✓ | ✓ | | ✓ | | ✓ |
| Balasundaram Jothi | ✓ | ✓ | | ✓ | ✓ | ✓ | | ✓ | | ✓ | | | ✓ | ✓ |

C : **C**onceptualization
M : **M**ethodology
So : **So**ftware
Va : **Va**lidation
Fo : **Fo**rmal analysis
I : **I**nvestigation
R : **R**esources
D : **D**ata Curation
O : Writing - **O**riginal Draft
E : Writing - Review & **E**diting
Vi : **Vi**sualization
Su : **Su**pervision
P : **P**roject administration
Fu : **Fu**nding acquisition

## CONFLICT OF INTEREST STATEMENT

Authors state no conflict of interest.

## DATA AVAILABILITY

The authors confirm that the data supporting the findings of this study are available within the article and its supplementary materials.

## REFERENCES


[1] J. Molins-Benlliure, M. Cabedo-Fabrés, E. Antonino-Daviu, and M. Ferrando-Bataller, "Miniaturized On-Ground 2.4 GHz IoT LTCC Chip Antenna and Its Positioning on a Ground Plane," *Sensors*, vol. 23, no. 6, pp. 1–16, 2023, doi: 10.3390/s23063007.

[2] A. Jabbar, M. A. Jamshed, Q. Abbasi, M. A. Imran, and M. Ur-Rehman, "Leveraging the Role of Dynamic Reconfigurable Antennas in Viewpoint of Industry 4.0 and Beyond," *Research*, vol. 6, 2023, doi: 10.34133/research.0110.

[3] S. K. Ibrahim *et al.*, "Design, Challenges and Developments for 5G Massive MIMO Antenna Systems at Sub 6-GHz Band: A Review," *Nanomaterials*, vol. 13, no. 3, pp. 1–40, 2023, doi: 10.3390/nano13030520.

[4] K. Çelik, "The Novel Monopole Antenna for Sub-6 GHz 5G Applications," *Gazi Üniversitesi Fen Bilimleri Dergisi Part C: Tasarım ve Teknoloji*, vol. 12, no. 3, pp. 579–584, 2024, doi: 10.29109/gujsc.1518514.

[5] S. Ellusamy and R. Balasubramanian, "Wideband circularly polarized reconfigurable metasurface antenna for 5G applications," *Frequenz*, vol. 78, no. 11–12, pp. 581–592, 2024, doi: 10.1515/freq-2023-0216.

[6] A. Khan, A. Ahmad, and M. Alam, "A High-Gain Reflector- DGS-Superstates -Enabled Quad-Band 5G-Antenna for mm-wave Applications," *Transactions on Electromagnetic Spectrum*, vol. 3, no. 1, pp. 34–50, 2023, doi: 10.5281/zenodo.8363039.

[7] S. N. R. Rizvi, W. A. Awan, and N. Hussain, "Design and Characterization of Miniaturized Printed Antenna for UWB Communication Systems," *Journal of Electrical Engineering and Technology*, vol. 16, no. 2, pp. 1003–1010, 2021, doi: 10.1007/s42835-020-00630-3.

[8] Y. Natali *et al.*, "Study on Defected Ground Structure Models with Miniaturized Patches for Broadband Wireless Systems," *Journal of Communications*, vol. 19, no. 3, pp. 168–174, 2024, doi: 10.12720/jcm.19.3.168-174.

[9] A. Kapoor, R. Mishra, A. Kapoor, and P. Kumar, "Compact wideband-printed antenna for Sub-6 GHz fifth-generation applications," *International Journal on Smart Sensing and Intelligent Systems*, vol. 13, no. 1, pp. 1–10, 2020, doi: 10.21307/ijssis-2020-033.

[10] M. A. Abdelghany, A. A. Ibrahim, H. A. Mohamed, and E. Tammam, "Compact Sub-6 GHz Four-Element Flexible Antenna for 5G Applications," *Electronics*, vol. 13, no. 3, pp. 1–18, 2024, doi: 10.3390/electronics13030537.

[11] A. Yumuşak and K. Çelik, "Metasurface-based MIMO Antenna Design and Analysis for 5G Communication Systems," *Transactions on Electromagnetic Spectrum*, vol. 4, no. 2, pp. 22–30, 2025.

[12] I. Ishteyaq, I. S. Masoodi, and K. Muzaffar, "A compact double-band planar printed slot antenna for Sub-6 GHz 5G wireless applications," *International Journal of Microwave and Wireless Technologies*, vol. 13, no. 5, pp. 469–477, Jun. 2021, doi: 10.1017/S1759078720001269.

[13] E. M. Ali, W. A. Awan, A. Abbas, S. M. Abbas, and H. G. Mohamed, "Compact Frequency-Agile and Mode-Reconfigurable Antenna for C-Band, Sub-6-GHz-5G, and ISM Applications," *Micromachines*, vol. 16, no. 6, pp. 1–15, 2025, doi: 10.3390/mi16060724.
[14] B. Tütüncü and M. Kösem, "Substrate Analysis on the Design of Wide-Band Antenna for Sub-6 GHz 5G Communication," *Wireless Personal Communications*, vol. 125, no. 2, pp. 1523–1535, 2022, doi: 10.1007/s11277-022-09619-9.
[15] N. Sheriff, S. Kamal, H. T. Chattha, T. K. Geok, and B. A. Khawaja, "Compact Wideband Four-Port MIMO Antenna for Sub-6 GHz and Internet of Things Applications," *Micromachines*, vol. 13, no. 12, pp. 1–11, 2022, doi: 10.3390/mi13122202.
[16] S. Islam, M. Zada, and H. Yoo, "Low-Pass Filter Based Integrated 5G Smartphone Antenna for Sub-6-GHz and mm-Wave Bands," *IEEE Transactions on Antennas and Propagation*, vol. 69, no. 9, pp. 5424–5436, 2021, doi: 10.1109/TAP.2021.3061012.
[17] S. Palanisamy, S. Nallusamy, N. Thangavelsamy, S. Guizani, and H. Hamam, "High-Performance Sub-6GHz 5G Antenna with Frequency Selective Surface Integration: Design, Optimization and Experimental Validation," *Traitement du Signal*, vol. 42, no. 4, pp. 1823–1839, Aug. 2025, doi: 10.18280/ts.420401.
[18] B. Sugumaran, R. Balasubramanian, and S. K. Palaniswamy, "Performance evaluation of compact FSS-integrated flexible monopole antenna for body area communication applications," *International Journal of Communication Systems*, vol. 35, no. 6, 2022, doi: 10.1002/dac.5085.
[19] R. Garg, P. Bhartia, I. Bahl, and A. Ittipiboon, *Microstrip antenna design handbook*. Norwood, MA, USA: Artech House, 2001.
[20] M. H. B. Ucar, A. Kazdag, and G. Çakır, "Miniature circular patch antenna design using defected ground structure based on complementary split-ring resonator for 5G wireless cellular networks," *Wireless Networks*, vol. 31, no. 5, pp. 3825–3842, 2025, doi: 10.1007/s11276-025-03968-6.
[21] C. Mohan, J. Silamboli, S. Divya, and R. S. Sheela, "A Compact Inset Coupled-Fed Triangular Patch Antenna For Wideband 5G Applications," *Indonesian Journal of Electrical Engineering and Informatics*, vol. 12, no. 3, pp. 659–666, 2024, doi: 10.52549/ijeei.v12i3.5677.
[22] M. A. Ullah, R. Keshavarz, M. Abolhasan, J. Lipman, and N. Shariati, "Low-profile dual-band pixelated defected ground antenna for multistandard IoT devices," *Scientific Reports*, vol. 12, no. 1, pp. 1–19, 2022, doi: 10.1038/s41598-022-15604-w.
[23] T. Saeidi, A. J. A. Al-Gburi, and S. Karamzadeh, "A Miniaturized Full-Ground Dual-Band MIMO Spiral Button Wearable Antenna for 5G and Sub-6 GHz Communications," *Sensors*, vol. 23, no. 4, pp. 1–30, 2023, doi: 10.3390/s23041997.
[24] N. A. Nafi, C. T. Israt, K. M. A. Rahman, N. D. Anik, and A. Rahman, "A novel theta-shaped slotted patch antenna with a unique DGS for Sub-6 GHz 5G communication," *Results in Engineering*, vol. 24, pp. 1–10, 2024, doi: 10.1016/j.rineng.2024.103506.
[25] A. Desai, T. Upadhyaya, J. Patel, R. Patel, and M. Palandoken, "Flexible CPW fed transparent antenna for WLAN and sub-6 GHz 5G applications," *Microwave and Optical Technology Letters*, vol. 62, no. 5, pp. 2090–2103, May 2020, doi: 10.1002/mop.32287.

## BIOGRAPHIES OF AUTHORS



**Arputham Jenifer** is an assistant professor in the Department of Artificial Intelligence and Data Science at St. Joseph's Institute of Technology, Chennai. She received her B.E. degree in Computer Science and Engineering from SRR Engineering College, Chennai, and her M.E. degree in Computer Science and Engineering from GKM College of Engineering and Technology, Chennai. She is currently pursuing research in the field of artificial intelligence. Her research interests include artificial intelligence, federated learning, medical image analysis, explainable AI, deep learning architectures, and healthcare automation, and ML-based device optimisation. She can be contacted at email: Jeni.8819@gmail.com.



**Chinnasamy Mohan** is working as assistant professor in Electronics and Communication Engineering, St. Joseph's Institute of Technology, Tamil Nadu, India. He has completed Ph.D. in planar antenna in the Department of Electronics and Communication Engineering at Sri Sivasubramaniya Nadar College of Engineering, Anna University, India. He received his B.E. in Electronics and Communication engineering from Peri Institute of Technology, Anna University, Chennai, Tamil Nadu, India in 2015 and his M.E. in Communication Systems in Sri Venkateshwara College of Engineering, Anna University, Chennai, Tamil Nadu, India in 2017. His research interests include are microwave components like antennas, metamaterials, and electromagnetic bandgap structures. He can be contacted at email: mohanrc803@gmail.com.



**Sasidharan Sandhya** is currently working as an assistant professor in the Department of Artificial Intelligence and Data Science at Easwari Engineering College, Ramapuram, Chennai. She has 4.9 years of academic experience. She received her B.Tech. degree in Information Technology from CSI Institute of Technology and her M.Tech. degree in Computer and Information Technology from Manonmaniam Sundaranar University. Her research interests include artificial intelligence, deep learning, image processing, and cyber security. She can be contacted at email: sandhya.check@gmail.com.



**Anbarasu Muthu Manickam** was born on September 4, 1979 in Thiruppathur, Tamilnadu, India. He completed his Bachelor's degree in Electronics and Communication Engineering from Mohamed Sathak Engineering College, Madurai Kamaraj University, Madurai in the year 2001. In continuous, he completed his M.E. degree in Communication Systems from K.L.N College of Engineering, Anna University, Chennai in the year 2007. As a golden achievement, he has completed his Ph.D. award in the field of RF and antenna from K.L.N College of Engineering, Anna University, Chennai. His research interests include antenna, optical communication, and MIMO systems. He can be contacted at email: muthumanicckam@gmail.com.



**Ravindran Sornalatha** is currently working as an associate professor in the Department of Electrical and Electronics Engineering at Mount Zion College of Engineering and Technology, Pudukkottai, Tamil Nadu, India. She completed her B.E. degree in 1996 from Arulmigu Kalasalingam College of Engineering, Madurai Kamaraj University, and her M.E. in VLSI Design in 2010 from Kings College of Engineering, Anna University, Trichy. She obtained her Ph.D. from the Faculty of Information and Communication Engineering, Anna University, Chennai, in 2021. She has 21 years of professional experience. She can be contacted at email: ravindransornalatha@gmail.com.



**Balasundaram Jothi** is currently working as assiociate professor in the Department of Computer Science and Engineering, SRM Institute of Science and Technology, Chennai, India. She received her doctoral degree from SRM University in 2022. Her research interests are IoT networks, data mining, and software engineering. She is also guiding UG and PG students in various research problems in the above mentioned areas. She has also published more than 35 papers in peer-reviewed journals and in various national and international conferences. She has published 3 patents grants. She can be contacted at email: jothib@srmist.edu.in.